to a local hub-centered frame, rather than formation flying of multiple spacecraft relative to the libration point.

Future work may involve the study of higher order contributions, such as terms which are quadratic in the hub motion about L_2, as well as deviations from the circular restricted problem.

ACKNOWLEDGMENTS

The authors thank Dr. Jesse Leitner of the Guidance, Navigation, and Control Office at NASA's Goddard Space Flight Center for sponsoring this work and earlier investigations. Dr. Shannon Coffey of the Naval Research Laboratory contributed additional funding.

REFERENCES

[1] R. W. Farquhar, "The Control and Use of Libration-Point Satellites," Goddard Space Flight Center, NASA TR R-346, September 1970.

[2] R. W. Farquhar, *et al.*, "Trajectories and Orbital Maneuvers for the First Libration-Point Satellite," *J. Guidance and Control*, Vol. 3, No. 6, November–December 1980, pp. 549–554.

[3] D. L. Richardson, "Periodic Orbits About the L_1 and L_2 Collinear Points in the Circular-Restricted Problem," Computer Sciences Corporation, CSC/TR-78/6002, March 1978.

[4] K. C. Howell, B. T. Barden, and M. W. Lo, "Application of Dynamical Systems Theory to Trajectory Design for a Libration Point Mission," *J. of the Astronautical Sciences*, Vol. 45, No. 2, April–June 1997, pp. 161–178.

[5] K. C. Howell, "Families of Orbits in the Vicinity of the Collinear Libration Points," *J. of the Astronautical Sciences*, Vol. 49, No. 1, January–March 2001, pp. 107–125.

[6] F. Y. Hsiao and D. J. Scheeres, "The Dynamics of Formation Flight About A Stable Trajectory," AAS/AIAA Spaceflight Mechanics Meeting, San Antonio, Texas, January 2002, Paper No. 02-189.

[7] K. C. Gendreau, W. C. Cash, A.F. Shipley, and N. White, "The MAXIM Pathfinder X-ray Interferometry Mission," SPIE Astronomical Telescopes and Instrumentation Conference, August 2002, Paper No. 4851-39.

[8] D. W. Dunham and D. P. Muhonen, "Tables of Libration-Point Parameters for Selected Solar System Objects," *J. of the Astronautical Sciences*, Vol. 49, No. 1, January–March 2001, pp. 197–217.

RELATIVE TRAJECTORY ANALYSIS OF DISSIMILAR FORMATION FLYING SPACECRAFT

Shankar K. Balaji* **and Adrian R. Tatnall†**

This paper deals with the differential acceleration effects on spacecraft formation flying. A mathematical model is developed to analyze relative trajectory of spacecraft in the presence of significant perturbative forces. The equations of relative coordinates are derived as a precise solution to the formation geometry problem and are valid for both close and long distance formation patterns and for rendezvous analysis. The coordinates of motion are propagated forward in time for identical and dissimilar spacecraft for different initial conditions. The results of this paper provide a physical insight into the actual behaviour of satellites in a cluster with differential drag-area.

Nomenclature

a – semi-major axis
$\bar{a}_r$ – acceleration along the position vector r
$\bar{a}_t$ – acceleration in the velocity vector direction
$\bar{a}_z$ – acceleration in the normal direction
a_s – mean distance of the Earth from the sun
c – speed of light in vacuum
C_d – coefficient of drag
e – eccentricity
$\bar{e}_r$ – unit vector along the satellite orbit radius vector direction
$\bar{e}_t$ – unit vector along the local horizontal direction
$\bar{e}_z$ – unit vector along the orbit normal direction
F – solar energy flux at the spacecraft
h – angular momentum
i – inclination
J_2 – geo potential coefficient representing Earth's Oblateness, $J_2 = 1082.64 \times 10^{-6}$
m – mass of spacecraft
M – Mean anomaly
n – Mean motion
p – semilatus rectum

* Ph.D. Candidate, Astronautics Research Group, University of Southampton, Highfield, Southampton SO17 1BJ, England. E-mail: spbalaji@soton.ac.uk.

† Senior Lecturer, Astronautics Research Group, University of Southampton, Highfield, Southampton SO17 1BJ, England. E-mail: art4@soton.ac.uk.

$\bar{R}$ – position vector of the satellite
r_e – Radius of earth, $r_e = 6371 \times 10^6 km$,
r_s - distance of the satellite from the sun
S – projected area of the spacecraft in the direction of motion
t – time
$[T_{ui\Omega}]_m$ – transformation matrix from frame $OXYZ$ to $OPQR$
$[T_{\Omega iu}]_d$ – transformation matrix from frame $(oxyz)_d$ to $OXYZ$
u – argument of latitude, $u = \theta + \omega$
Ω – right ascension
ω – argument of perigee
θ – true anomaly
μ – gravitational earth constant, $\mu = 3.986 \times 10^{14} m^3/s^2$
ε – obliquity of the ecliptic
$\lambda_\odot$ – ecliptic longitude of the sun
ξ – constant of surface reflection

Subscripts
d – refers to the deputy satellite
m – refers to the master satellite
0 – refers to the initial conditions

INTRODUCTION

Spacecraft flying in formation need not be necessarily identical. There is always a possibility of some drag area difference due to technical requirements like antenna pointing. Even a small difference in drag area will contribute to a significant secular growth of distance between the satellites in a constellation. Some authors have even considered this to be an advantage and have proposed special drag surfaces on spacecraft to control or reconfigure a Formation pattern[7].

There are now plans to use small inspector or Escort satellites to perform visual and thermal imaging of a Chief-target satellite. This enables diagnosis for repair in the case of a breakdown and anticipates any malfunctions for similar missions. The relative trajectory of the escort satellite around the target would entirely depend on the difference in drag area and the altitude of their orbits.

In this paper, we will analyze the relative trajectory of formation flying spacecraft with small differential drag-Area using a mathematical model developed in the following sections. The relative coordinates of the spacecraft are derived by a series of transformations and translations from the Earth-centred inertial frame to the spacecraft-centred rotating frame. Dynamical force models like J_2, atmospheric drag and solar radiation pressure are then introduced into the equations in order to obtain a realistic

simulation model. The coordinates of motion are then propagated forward in time with different initial conditions. The Equations for the relative coordinates are derived as a precise solution to the Formation geometry problem and, unlike the traditional Clohessy-Wiltshire[11] equations for relative trajectory analysis, impose no restrictions on eccentricity of the orbits of the spacecraft investigated. The equations are valid both for close and long distance formation-flying patterns and for rendezvous analysis. The results of this paper provide a physical insight into the actual behaviour of satellites in a cluster with a differential drag-Area. The assessment of the relative trajectory is imperative for selecting the actuators for station keeping, designing control laws and deciding the configuration of the spacecraft.

MATHEMATICAL MODELLING OF RELATIVE MOTION

The equations for the relative coordinates are derived as a precise solution to the formation geometry problem with the definition of orbital frames and orbital elements as shown in Figure 1. We will hereafter denote the reference satellite as the master satellite (subscript m) and the satellite to be observed as the deputy (subscript d). It should be noted that there could be many deputy spacecraft for a specific mission. But in our case we will assume that the formation consists of only two spacecraft namely the master and the deputy.

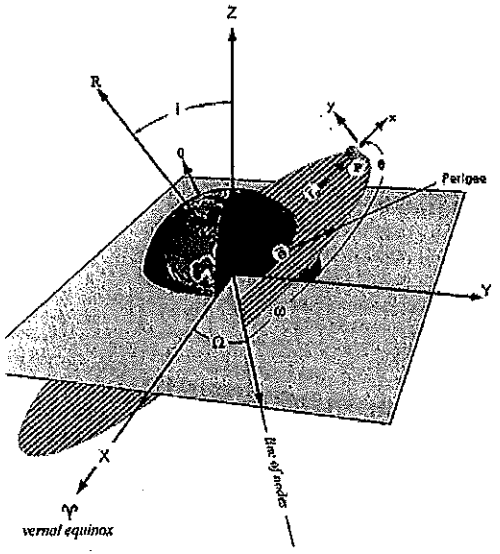

Figure 1 – Orbital Frames and elements

The origin of the spacecraft centered co-ordinate system is assumed to be at the master satellite's centre of mass. The origin of the coordinate system $OXYZ$ is at the center of

the earth with the XY plane coinciding with the Earth's equatorial plane and X-axis pointing in the direction of vernal eqinox γ. The Z-axis points in the direction of the North Pole and the Y-axis is normal to the XZ plane and completes the right-handed frame of system. The origin of the system $OPQR$ also lies at the center of the earth with the P axis pointing in the direction of the master satellite's Centre-of-Mass. The unit vector of P is defined as

$$P = \frac{r}{|r|} \tag{1}$$

where r is the radius vector of the spacecraft. The Q-axis points in the direction of the angular velocity of the orbital plane (normal to the orbit) and R-axis completes the right-handed frame of system. The origin of the $oxyz$ system lies at the master satellite's center of mass and its unit vectors are

$$x = P, \qquad y = Q, \qquad z = R \tag{2}$$

Frame XYZ axes can be transformed to frame PQR axes by 3 successive rotations that are as follows:

1. Rotation about the Z axis by $+\Omega$
2. Rotation about the X axis by $+i$
3. Rotation about the Z axis by $+u$ $(u = \omega + \theta)$

The new coordinates can now be represented as

$$\begin{bmatrix} P \\ Q \\ R \end{bmatrix} = \left[T_{ui\Omega}\right]_m \begin{bmatrix} X \\ Y \\ Z \end{bmatrix} \tag{3}$$

Where

$$\left[T_{ui\Omega}\right]_m = \begin{bmatrix} \cos u_m & \sin u_m & 0 \\ -\sin u_m & \cos u_m & 0 \\ 0 & 0 & 1 \end{bmatrix} \bullet \begin{bmatrix} 1 & 0 & 0 \\ 0 & \cos i_m & \sin i_m \\ 0 & -\sin i_m & \cos i_m \end{bmatrix} \bullet \begin{bmatrix} \cos\Omega_m & \sin\Omega_m & 0 \\ -\sin\Omega_m & \cos\Omega_m & 0 \\ 0 & 0 & 1 \end{bmatrix} \tag{4}$$

The coordinates of the deputy spacecraft (from Eq.(3)) in the OPQR system are

$$\begin{bmatrix} P_d \\ Q_d \\ R_d \end{bmatrix} = \left[T_{ui\Omega}\right]_m \begin{bmatrix} X_d \\ Y_d \\ Z_d \end{bmatrix} \tag{5}$$

The Coordinates X_d, Y_d, Z_d can also be represented by the Matrix as given below

$$\begin{bmatrix} X_d \\ Y_d \\ Z_d \end{bmatrix} = \left[T_{\Omega iu}\right]_d \begin{bmatrix} R_d \\ 0 \\ 0 \end{bmatrix} \tag{6}$$

Where

$$\left[T_{\Omega iu}\right]_d = \begin{bmatrix} \cos\Omega_d & -\sin\Omega_d & 0 \\ \sin\Omega_d & \cos\Omega_d & 0 \\ 0 & 0 & 1 \end{bmatrix} \bullet \begin{bmatrix} 1 & 0 & 0 \\ 0 & \cos i_d & -\sin i_d \\ 0 & \sin i_d & \cos i_d \end{bmatrix} \bullet \begin{bmatrix} \cos u_d & -\sin u_d & 0 \\ \sin u_d & \cos u_d & 0 \\ 0 & 0 & 1 \end{bmatrix} \tag{7}$$

Substituting Eq.(6) in Eq.(5),we get the Coordinates X_d, Y_d, Z_d in the OPQR frame as

$$\begin{bmatrix} P \\ Q \\ R \end{bmatrix} = \left[T_{ui\Omega}\right]_m \bullet \left[T_{\Omega iu}\right]_d \bullet \begin{bmatrix} R_d \\ 0 \\ 0 \end{bmatrix} \tag{8}$$

Now shifting the origin of the OPQR frame to the master satellite's Centre-of-mass gives us the relative coordinates of the deputy spacecraft with respect to the master spacecraft in the oxyz frame.

$$\begin{bmatrix} x \\ y \\ z \end{bmatrix} = \left[T_{ui\Omega}\right]_m \bullet \left[T_{\Omega iu}\right]_d \bullet \begin{bmatrix} R_d \\ 0 \\ 0 \end{bmatrix} - \begin{bmatrix} R_m \\ 0 \\ 0 \end{bmatrix} \tag{9}$$

Combining the two transformations in to one then gives

$$\begin{bmatrix} x \\ y \\ z \end{bmatrix} = [A] \bullet \begin{bmatrix} R_d \\ 0 \\ 0 \end{bmatrix} - \begin{bmatrix} R_m \\ 0 \\ 0 \end{bmatrix} \tag{10}$$

where $[A] = \left[T_{ui\Omega}\right]_m \bullet \left[T_{\Omega iu}\right]_d$ and $[A] = \begin{bmatrix} A_{11} & A_{12} & A_{13} \\ A_{21} & A_{22} & A_{23} \\ A_{31} & A_{32} & A_{33} \end{bmatrix}$

The elements of matrix A are given in the appendix 1 of this paper.

After evaluating the Left hand side terms of Eq.(10), we get the coordinates of the deputy spacecraft relative to the master spacecraft in xyz frame, at any time t, as

$$
\begin{aligned}
x(t) = {} & (cu_m(t)\cdot c\Omega_m(t)\cdot c\Omega_d(t)\cdot cu_d(t) - cu_m(t)\cdot c\Omega_m(t)\cdot s\Omega_d(t)\cdot ci_d(t)\cdot su_d(t) \\
& -su_m(t)\cdot ci_m(t)\cdot s\Omega_m(t)\cdot c\Omega_d(t)\cdot cu_d(t) + su_m(t)\cdot ci_m(t)\cdot s\Omega_m(t)\cdot s\Omega_d(t)\cdot ci_d(t)\cdot su_d(t) \\
& +cu_m(t)\cdot s\Omega_m(t)\cdot s\Omega_d(t)\cdot cu_d(t) + cu_m(t)\cdot s\Omega_m(t)\cdot c\Omega_d(t)\cdot ci_d(t)\cdot su_d(t) \\
& +su_m(t)\cdot ci_m(t)\cdot c\Omega_m(t)\cdot s\Omega_d(t)\cdot cu_d(t) + su_m(t)\cdot ci_m(t)\cdot c\Omega_m(t)\cdot c\Omega_d(t)\cdot ci_d(t)\cdot su_d(t) \\
& +su_m(t)\cdot si_m(t)\cdot si_d(t)\cdot su_d(t))\cdot R_d(t) - R_m(t) \\
y(t) = {} & (-su_m(t)\cdot c\Omega_m(t)\cdot c\Omega_d(t)\cdot cu_d(t) + su_m(t)\cdot c\Omega_m(t)\cdot s\Omega_d(t)\cdot ci_d(t)\cdot su_d(t) \\
& -cu_m(t)\cdot ci_m(t)\cdot s\Omega_m(t)\cdot c\Omega_d(t)\cdot cu_d(t) + cu_m(t)\cdot ci_m(t)\cdot s\Omega_m(t)\cdot s\Omega_d(t)\cdot ci_d(t)\cdot su_d(t) \\
& -su_m(t)\cdot s\Omega_m(t)\cdot s\Omega_d(t)\cdot cu_d(t) - su_m(t)\cdot s\Omega_m(t)\cdot c\Omega_d(t)\cdot ci_d(t)\cdot su_d(t) \\
& +cu_m(t)\cdot ci_m(t)\cdot c\Omega_m(t)\cdot s\Omega_d(t)\cdot cu_d(t) + cu_m(t)\cdot ci_m(t)\cdot c\Omega_m(t)\cdot c\Omega_d(t)\cdot ci_d(t)\cdot su_d(t) \\
& +cu_m(t)\cdot si_m(t)\cdot si_d(t)\cdot su_d(t))\cdot R_d(t) \\
z(t) = {} & (si_m(t)\cdot s\Omega_m(t)\cdot c\Omega_d(t)\cdot cu_d(t) - si_m(t)\cdot s\Omega_m(t)\cdot s\Omega_d(t)\cdot ci_d(t)\cdot su_d(t) \\
& -si_m(t)\cdot c\Omega_m(t)\cdot s\Omega_d(t)\cdot cu_d(t) - si_m(t)\cdot c\Omega_m(t)\cdot c\Omega_d(t)\cdot ci_d(t)\cdot su_d(t) \\
& +su_d(t)\cdot si_d(t)\cdot ci_m(t))\cdot R_d(t)
\end{aligned}
\qquad (11)
$$

where $R_m(t) = \dfrac{a_m(t)\cdot(1-e_m(t)^2)}{1+e_m(t)\cdot\cos\theta_m(t)}$ and $R_d(t) = \dfrac{a_d(t)\cdot(1-e_d(t)^2)}{1+e_d(t)\cdot\cos\theta_d(t)}$

c and s in Eq.(11) represent cosine and sine functions respectively.

Since Eq.(11) has all the orbital properties of both the master and deputy satellites, it can be used to analyze any type of formation pattern with any number of satellites acting as the deputy.

At any time t, the value of any orbital element under the influence of perturbative forces can be found out from the following equations.

$$
\begin{aligned}
& a(t) = a(t_0) + \int_{t_0}^{t} \frac{da}{dt}\cdot dt \qquad e(t) = e(t_0) + \int_{t_0}^{t} \frac{de}{dt}\cdot dt \qquad i(t) = i(t_0) + \int_{t_0}^{t} \frac{di}{dt}\cdot dt \\
& \Omega(t) = \Omega(t_0) + \int_{t_0}^{t} \frac{d\Omega}{dt}\cdot dt \qquad \omega(t) = \omega(t_0) + \int_{t_0}^{t} \frac{d\omega}{dt}\cdot dt \qquad M(t) = M(t_0) + \int_{t_0}^{t} \frac{dM}{dt}\cdot dt
\end{aligned}
\qquad (12)
$$

Eq.(12), when substituted in Eq.(11) with respective subscripts m and d, portray the relative trajectory of any deputy satellite as seen from the master satellite.

Gauss equations can be used to find the rate of change of orbital elements in Eqn.(12). The Gauss perturbation equations are a group of equations that describe the change of all orbital elements with time in the presence of perturbations. They are well suited to study long-term evolution of orbital elements under perturbation influence[9]. The Gauss perturbation equations are given as;

$$
\begin{aligned}
& \frac{da}{dt} = \frac{2e\sin\theta}{nx}a_r + \frac{2ax}{nr}a_t \\
& \frac{de}{dt} = \frac{x\sin\theta}{na}a_r + \frac{x}{na^2e}\left(\frac{a^2x^2}{r} - r\right)a_t \\
& \frac{di}{dt} = \frac{r\cos u}{na^2x}a_z \\
& \frac{d\Omega}{dt} = \frac{r\sin u}{na^2x\sin i}a_z \\
& \frac{d\omega}{dt} = \frac{x\cos\theta}{nae}a_r + \frac{p}{eh}\left[\sin\theta\left(1+\frac{1}{1+e\cos\theta}\right)\right]a_t - \frac{r\cot i\sin u}{na^2x}a_z \\
& \frac{dM}{dt} = n - \frac{1}{na}\left(\frac{2r}{a} - \frac{x^2}{e}\cos\theta\right)a_r - \frac{x^2}{nae}\left(1+\frac{r}{ax^2}\right)\sin\theta a_t
\end{aligned}
\qquad (13)
$$

where $x = \sqrt{1-e^2}$, $u = \omega + \theta$, $p = a(1-e^2)$, $h = \sqrt{\mu p}$

The overall rate of change of orbital elements due to perturbing accelerations like Atmospheric drag, Solar radiation pressure and J_2 can be found by introducing their acceleration components in the gauss equations.

MODELLING OF EXTERNAL FORCES

The following perturbing accelerations are modeled in the simulation.

Drag: The magnitude of acceleration induced by atmospheric drag depends on the altitude of the satellite orbit and to a great extent depends on the satellite's surface area and mass. The drag deceleration can be written as

$$a_{drag} = \frac{C_d S \rho V^2}{2m} \qquad (14)$$

Unlike other perturbative forces, drag force has acceleration component only along the negative velocity vector direction.

Solar radiation pressure: The perturbing acceleration of an earth satellite due to solar radiation pressure effects can be computed with the following equation.

$$a_{SRP} = \xi\frac{A}{m}SRP\left(\frac{a_s}{r_s}\right)^2 \qquad (15)$$

Where SRP = F / c

The components of Solar-radiation pressure can be expressed as [9].

$$\begin{Bmatrix} e_r \\ e_t \end{Bmatrix} = \cos^2\frac{i}{2}\cos^2\frac{\varepsilon}{2}\begin{Bmatrix}\cos\\ \sin\end{Bmatrix}(\lambda_\odot - u - \Omega) - \sin^2\frac{i}{2}\sin^2\frac{\varepsilon}{2}\begin{Bmatrix}\cos\\ \sin\end{Bmatrix}(\lambda_\odot - u + \Omega)$$
$$-\frac{1}{2}\sin i\sin\varepsilon\left[\begin{Bmatrix}\cos\\ \sin\end{Bmatrix}(\lambda_\odot - u) - \begin{Bmatrix}\cos\\ \sin\end{Bmatrix}(-\lambda_\odot - u)\right]$$
$$-\sin^2\frac{i}{2}\cos^2\frac{\varepsilon}{2}\begin{Bmatrix}\cos\\ \sin\end{Bmatrix}(-\lambda_\odot - u + \Omega) - \cos^2\frac{i}{2}\sin^2\frac{\varepsilon}{2}\begin{Bmatrix}\cos\\ \sin\end{Bmatrix}(-\lambda_\odot - u - \Omega)$$

$$e_z = \sin i\cos^2\frac{\varepsilon}{2}\sin(\lambda_\odot - \Omega) - \sin i\sin^2\frac{\varepsilon}{2}\sin(\lambda_\odot + \Omega) - \cos i\sin\varepsilon\sin\lambda_\odot \qquad (16)$$

The quantities ε, $\lambda_\odot$ and a_s/r_s (in Eq.(16)) can be computed with sufficient accuracy from the following expressions[12]

$d = MJD - 15019.5$, Modified Julian Day (MJD) = Julian day - 2400000.5

$\varepsilon = 23^\circ.44$

$M_\odot = 358^\circ.48 + 0^\circ.98560027d$

$\lambda_\odot = 279^\circ.70 + 0^\circ.9856473d + 1^\circ.92\sin M_\odot$

$a_s / r_s = [1 + 0.01672\cos(M_\odot + 1^\circ.92\sin M_\odot)]/0.99972$

Oblateness of earth: J_2 is related to Earth equatorial oblateness through earth rotation, and the estimated difference between the polar radius and equatorial radius is 22 km. The zonal harmonic J_2 is responsible for the secular rates of the right ascension of the ascending node Ω, the argument of perigee ω, and a small correction to the mean motion of the orbit. J_2 induced accelerations can be given in the spherical coordinate system as[9].

$$\bar{a}_{j_2} = -\frac{3J_2\mu r_e^4}{r^4}[\bar{e}_r(0.5 - 1.5\sin^2 i\sin^2 u) + \bar{e}_t\sin^2 i\sin u\cos u + \bar{e}_z\sin i\cos i\sin u] \qquad (17)$$

SIMULATION AND RESULTS

Based on the mathematical model developed in the previous sections, numerical simulations of relative motion are presented for different test cases of the Leader-Follower formation pattern. As the name implies, the Leader-Follower configuration has satellites lying on the same orbital plane and separated only by mean anomaly. Simulations are conducted for the leader-follower pattern at 600 km and 800 km near-circular, polar orbits. The separation distance of the spacecraft for all the test cases is initialised to 1000 meters. Test cases are simulated with 0%, 5% and 10% more drag area for the deputy satellite than the master satellite. In order to isolate the effect of

various forces, simulations are carried out with and without solar radiation pressure and J_2. In all the test cases, atmospheric drag is considered to be the principal perturbing factor. The differential solar radiation pressure effects are also modelled in the simulations. In the calculations for drag and solar radiation pressure the normal drag-area of the satellites is assumed to be 0.1225 m^2 and the drag coefficient C_d =2.2. The summary of initial conditions used for simulation is given below

Epoch:	1st January 2004
Orbit altitude:	600 km and 800 km
Type:	Circular and Polar
Perturbations:	Atmospheric drag, Solar radiation pressure, J_2
Atmosphere:	Jacchia Roberts
Numerical method:	Rung-Kutta Fehlberg 8th order
Initial step size:	1 second
Propagation duration:	1 orbit
Physical properties:	Mass=25 kg, C_d =2.2, Surface-area=0.1225 m^2
Initial separation:	1000 metres

Figure 2 portrays the relative motion of the identical spacecraft in the *xy* plane with all perturbing factors including drag, solar radiation pressure and J_2 for one complete orbit. It can be seen that the relative motion is a 2 x 1 ellipse with the ellipse spiraling inwards with time. The cause of oscillations in the radial, along-track and cross-track directions can be attributed to J_2. The amplitude of the oscillations is in the order of few meters for the along-track and radial directions and a few millimeters for the cross-track direction. J_2 also induces a minor drift of a few centimeters/orbit in both the along track and radial directions. Due to the spacecraft being identical in cross-section area, there is no drift caused by atmospheric drag and this was verified by disengaging J_2 from the simulation. The blue solid line in figures 3-6 is the trajectory of the deputy satellite in the *xy* plane with 5% more differential drag area than the master satellite. The red dotted lines in the figures represent the trajectory for 10% more differential drag area. Figures 3 and 5 illustrate the relative motion in the presence of solar radiation pressure and drag with no J_2 effects for 600 km and 800 km altitudes respectively for 1 complete orbit. The 5% differential area caused a net secular drift of 19 cm/orbit, in the along-track direction, for the 600 km altitude and 0.75 cm/orbit for the 800 km altitude. The total drifts doubled in magnitude with the doubling of the differential drag area. Figures 4 and 6 represent the trajectory simulated only with atmospheric drag for 1 complete orbit. It can be seen that the net drift in the along-track direction for such a test case is 22 cm/orbit for the 600 km altitude and 2.5 cm/orbit for the 800 km altitude. The values doubled for 10% differential drag area.

It is also interesting to note that the inclusion of differential solar radiation pressure effects in the model actually reduces the total drift caused by differential drag by a few centimeters. Solar radiation pressure causes the spacecraft to accelerate or decelerate depending upon whether the spacecraft is moving towards or away from the sun. This effect when combined with the differential area effects causes a decrease in the net secular drift. The solar radiation pressure effects also vary for different types of orbits, for different altitudes and for different periods of the year. The comparison of figures 3

and 5 shows that solar radiation pressure has significant effects on the satellite relative motion at higher altitudes. Although in the figures 2-6, the along track displacement seems to increase with the progress of the orbit, it actually decreases and the value shown in the figures are just an absolute value of the original value. Due to the reason that the deputy spacecraft has more drag area than the master spacecraft, it dissipates more kinetic energy into heat through drag than the master. The decrease in the orbital velocity of the deputy satellite slows it and makes it enter an elliptic inward spiral. As it looses height, it starts to accelerate and tries to catch up with the master spacecraft if its motion is not controlled. Based on the simulation values, the ΔV required to compensate for the secular drifts in the along-track and radial directions are 0.5 m/sec/year for 5% drag area difference for the 600 km altitude and 0.08 m/sec/year for 5% drag area difference for the 800 km altitude. The values are twice the values of 5% for 10% drag area difference. It should be noted that these values are just a rough conservative estimate of the ΔV requirements only to compensate the differential drag effect.

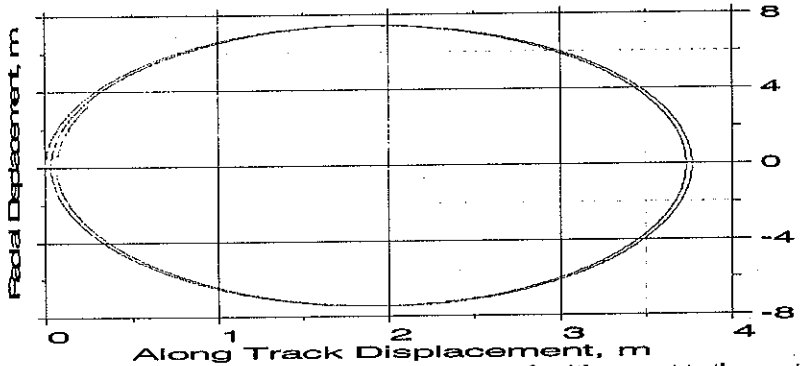

Figure 2 Relative motion of the deputy spacecraft with respect to the master spacecraft in the xy plane with zero percent differential drag area and in the presence of atmospheric drag, solar radiation pressure and J_2 for 600 km altitude

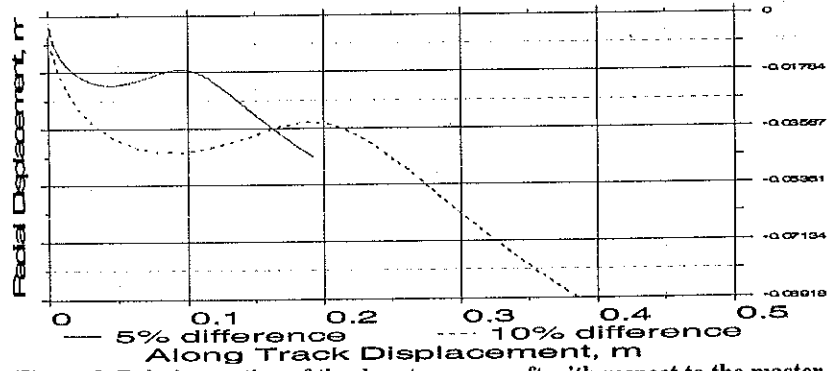

Figure 3. Relative motion of the deputy spacecraft with respect to the master spacecraft in the *xy* plane with 5% and 10% differential drag area with atmospheric drag and solar radiation pressure and ignoring J_2 for 600 km altitude

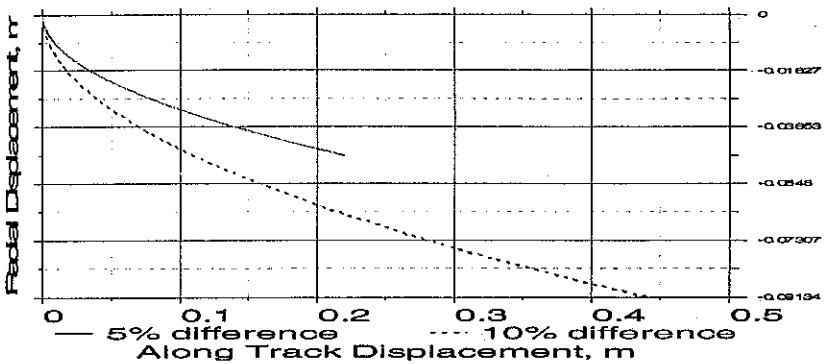

Figure 4. Relative motion of the deputy spacecraft with respect to the master spacecraft in the *xy* plane with 5% and 10% differential drag area with atmospheric drag and ignoring solar radiation pressure and J_2 for 600 km altitude

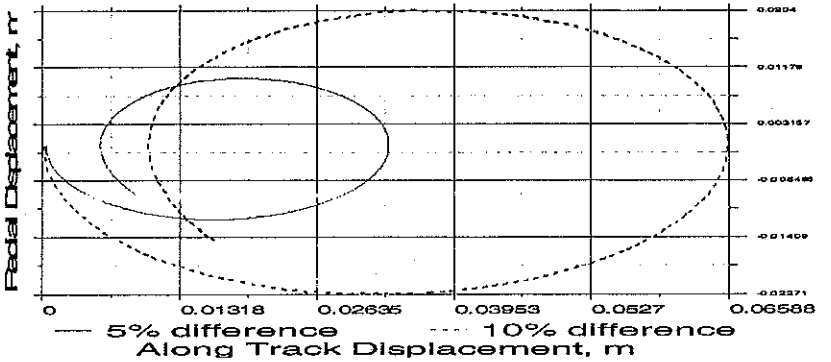

Figure 5. Relative motion of the deputy spacecraft with respect to the master spacecraft in the *xy* plane with 5% and 10% differential drag area with atmospheric drag and solar radiation pressure and ignoring J_2 for 800 km altitude

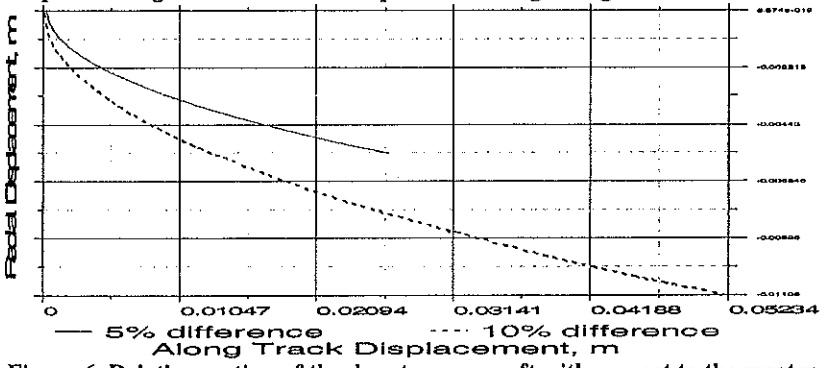

Figure 6. Relative motion of the deputy spacecraft with respect to the master spacecraft in the *xy* plane with 5% and 10% differential drag area with atmospheric drag and solar radiation pressure and ignoring J_2 for 800 km altitude

CONCLUSION

In this paper, we develop a precise mathematical model to analyze the relative trajectory of formation flying spacecraft. The equations for relative motion are derived using the geometry of the formation-flying problem. Based on the mathematical model, the relative trajectory is simulated for the leader follower formation pattern for two different altitudes and for two different differential drag values. Spacecraft relative motion is compared and analyzed for different force conditions. Finally, the ΔV requirements are estimated for the secular drifts induced by the differential drag effects. The mathematical developed in this paper can be used to analyze the relative trajectory of any type of formation configuration with any number of spacecraft.

REFERENCES

1. K.T.Alfriend, H. Schaub, and D.W.Gim, "Gravitational Perturbations, Non-linearity and Circular Orbit Assumption Effects on Formation Flying Control Strategies", Paper No. AAS 00-012, *23rd Annual AAS Guidance and Control Conference*, Breckenridge, CO, Feb. 2000.
2. R.G. Melton, "Time-Explicit representation of relative Motion Between Elliptical Orbits," *AAS/AIAA Astrodynamics Specialists Conference,* Sun valley, ID, Aug.1997.
3. Hans.F.Meissinger, "Low-cost, minimum-size satellites for demonstration of formation flying modes at small, kilometer-size distances," *13th AIAA/USU Conference on Small Satellites*, 1999.
4. D.W.Gim, and K.T. Alfriend., "The State Transition Matrix of Relative Motion for the Perturbed Non-Circular Reference Orbit", *2001 AAS/AIAA Space Flight Mechanics Meeting*, Feb. 11-16, 2001, Santa Barbara.
5. Chris Sabol, Rich Burns and Craig A. McLaughlin, " Satellite Formation Flying Design and Evolution", *Journal of Spacecraft and Rockets*, Vol. 38, No. 2. Mar.-Apr. 2001.
6. David F. Chichka, " Satellite Clusters with Constant Apparent Distribution", *Journal of Guidance, Control, and Dynamics*, Vol. 24, No. 1. Jan.-Feb. 2001.
7. C.L.Leonard, " Orbital Formation-Keeping with Differential Drag", *Journal of Guidance, Control, and Dynamics*, Vol. 12, No. 1. Jan.-Feb. 1989.
8. R.H.Battin, " An introduction to the Mathematics and Methods of astrodynamics", *AIAA Education series*, Washington D.C. 1987.
9. Vladimir.A.Chobotov, "Orbital Mechanics Second edition ", *AIAA Education series*, Washington D.C. 1996
10. T.W. Williams and Z. S. Wang, "Potential Uses of Solar Radiation Pressure in Satellite Formation Flight", *10th AAS/AIAA Space Flight Mechanics Meeting*, Clearwater, FL, Jan. 2000
11. Clohessy, W. H. and Wiltshire, R. S., "Terminal Guidance System for Satellite Rendezvous," *Journal of the Aerospace Sciences*, Vol. 27, No. 5, 1960, pp. 653–658, 674.
12. Explanatory Supplement to the Astronomical Ephemeris, 1961, p.98.

APPENDIX 1

$$[A]=\left[T_{ui\Omega}\right]_m\cdot\left[T_{\Omega iu}\right]_d \quad \text{and} \quad [A]=\begin{bmatrix} A_{11} & A_{12} & A_{13} \\ A_{21} & A_{22} & A_{23} \\ A_{31} & A_{32} & A_{33} \end{bmatrix}$$

$$\begin{aligned} A_{11} = {} & cu_m\cdot c\Omega_m\cdot c\Omega_d\cdot cu_d - cu_m\cdot c\Omega_m\cdot s\Omega_d\cdot ci_d\cdot su_d - su_m\cdot ci_m\cdot s\Omega_m\cdot c\Omega_d\cdot cu_d \\ & + su_m\cdot ci_m\cdot s\Omega_m\cdot s\Omega_d\cdot ci_d\cdot su_d + cu_m\cdot s\Omega_m\cdot s\Omega_d\cdot cu_d + cu_m\cdot s\Omega_m\cdot c\Omega_d\cdot ci_d\cdot su_d \\ & + su_m\cdot ci_m\cdot c\Omega_m\cdot s\Omega_d\cdot cu_d + su_m\cdot ci_m\cdot c\Omega_m\cdot c\Omega_d\cdot ci_d\cdot su_d + su_m\cdot si_m\cdot si_d\cdot su_d \end{aligned}$$

$$\begin{aligned} A_{12} = {} & -cu_m\cdot c\Omega_m\cdot c\Omega_d\cdot su_d - cu_m\cdot c\Omega_m\cdot s\Omega_d\cdot ci_d\cdot cu_d + su_m\cdot ci_m\cdot s\Omega_m\cdot c\Omega_d\cdot su_d \\ & + su_m\cdot ci_m\cdot s\Omega_m\cdot s\Omega_d\cdot ci_d\cdot cu_d - cu_m\cdot s\Omega_m\cdot s\Omega_d\cdot su_d + cu_m\cdot s\Omega_m\cdot c\Omega_d\cdot ci_d\cdot cu_d \\ & - su_m\cdot ci_m\cdot c\Omega_m\cdot s\Omega_d\cdot su_d + su_m\cdot ci_m\cdot c\Omega_m\cdot c\Omega_d\cdot ci_d\cdot cu_d + su_m\cdot si_m\cdot si_d\cdot cu_d \end{aligned}$$

$$\begin{aligned} A_{13} = {} & c\Omega_m\cdot s\Omega_d\cdot si_d\cdot cu_m - s\Omega_d\cdot si_d\cdot su_m\cdot ci_m\cdot s\Omega_m - c\Omega_d\cdot s\Omega_m\cdot si_d\cdot cu_m \\ & - c\Omega_d\cdot si_d\cdot su_m\cdot ci_m\cdot c\Omega_m + su_m\cdot si_m\cdot ci_d \end{aligned}$$

$$\begin{aligned} A_{21} = {} & -su_m\cdot c\Omega_m\cdot c\Omega_d\cdot cu_d + su_m\cdot c\Omega_m\cdot s\Omega_d\cdot ci_d\cdot su_d - cu_m\cdot ci_m\cdot s\Omega_m\cdot c\Omega_d\cdot cu_d \\ & + cu_m\cdot ci_m\cdot s\Omega_m\cdot s\Omega_d\cdot ci_d\cdot su_d - su_m\cdot s\Omega_m\cdot s\Omega_d\cdot cu_d - su_m\cdot s\Omega_m\cdot c\Omega_d\cdot ci_d\cdot su_d \\ & + cu_m\cdot ci_m\cdot c\Omega_m\cdot s\Omega_d\cdot cu_d + cu_m\cdot ci_m\cdot c\Omega_m\cdot c\Omega_d\cdot ci_d\cdot su_d + cu_m\cdot si_m\cdot si_d\cdot su_d \end{aligned}$$

$$\begin{aligned} A_{22} = {} & su_m\cdot c\Omega_m\cdot c\Omega_d\cdot su_d + su_m\cdot c\Omega_m\cdot s\Omega_d\cdot ci_d\cdot cu_d + cu_m\cdot ci_m\cdot s\Omega_m\cdot c\Omega_d\cdot su_d \\ & + cu_m\cdot ci_m\cdot s\Omega_m\cdot s\Omega_d\cdot ci_d\cdot cu_d + su_m\cdot s\Omega_m\cdot s\Omega_d\cdot su_d - su_m\cdot s\Omega_m\cdot c\Omega_d\cdot ci_d\cdot cu_d \\ & - cu_m\cdot ci_m\cdot c\Omega_m\cdot s\Omega_d\cdot su_d + cu_m\cdot ci_m\cdot c\Omega_m\cdot c\Omega_d\cdot ci_d\cdot cu_d + cu_m\cdot si_m\cdot si_d\cdot cu_d \end{aligned}$$

$$\begin{aligned} A_{23} = {} & -c\Omega_m\cdot s\Omega_d\cdot si_d\cdot su_m - s\Omega_d\cdot si_d\cdot cu_m\cdot ci_m\cdot s\Omega_m + c\Omega_d\cdot s\Omega_m\cdot si_d\cdot su_m \\ & - c\Omega_d\cdot si_d\cdot cu_m\cdot ci_m\cdot c\Omega_m + cu_m\cdot si_m\cdot ci_d \end{aligned}$$

$$\begin{aligned} A_{31} = {} & si_m\cdot s\Omega_m\cdot c\Omega_d\cdot cu_d - si_m\cdot s\Omega_m\cdot s\Omega_d\cdot ci_d\cdot su_d - si_m\cdot c\Omega_m\cdot s\Omega_d\cdot cu_d \\ & - si_m\cdot c\Omega_m\cdot c\Omega_d\cdot ci_d\cdot su_d + su_d\cdot si_d\cdot ci_m \end{aligned}$$

$$\begin{aligned} A_{32} = {} & -si_m\cdot s\Omega_m\cdot c\Omega_d\cdot su_d - si_m\cdot s\Omega_m\cdot s\Omega_d\cdot ci_d\cdot cu_d + si_m\cdot c\Omega_m\cdot s\Omega_d\cdot su_d \\ & - si_m\cdot c\Omega_m\cdot c\Omega_d\cdot ci_d\cdot cu_d + cu_d\cdot si_d\cdot ci_m \end{aligned}$$

$$A_{33} = si_m\cdot s\Omega_m\cdot s\Omega_d\cdot si_d + si_m\cdot c\Omega_m\cdot c\Omega_d\cdot si_d + ci_d\cdot ci_m$$

where s and c represent sine and cosine functions respectively.